中国科学院高能物理研究所
Institute of High Energy Physics, Chinese Academy of Sciences

Leptonic PeVatrons

Dmitry Khangulyan
IHEP(Beijing) CRRC(Chengdu)

Cosmic Rays and Neutrinos in the Multi-Messanger Era
Paris (Dec 9th – 13th, 2024)


29°21′27.6″N
100°08′19.6″E
@4410m a.s.l.
WCDA:
1 – 20 TeV
78,000m²
KM2A:
10 – 10³ TeV
1188MDs
5612ED
WFCTA:
CR spec-
trometer
> 10 TeV
18 tele-
scopes

29°21′27.6″N
100°08′19.6″E
@4410m a.s.l.

WCDA:
1 – 20 TeV
78,000m^2

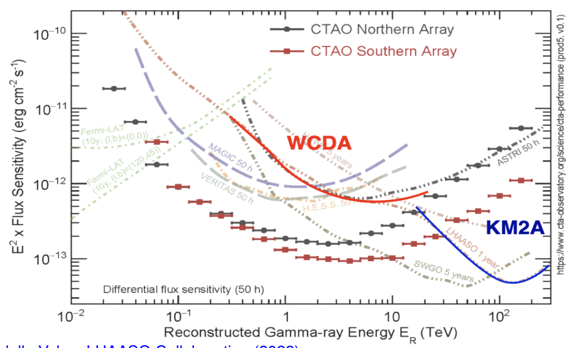

della Volpe, LHAASO Collaboration (2022)

KM2A:
10 – 10^3 TeV
1188MDs
5612ED

WFCTA:
CR spec-
trometer
$>$ 10 TeV
18 tele-
scopes

29°21′27.6″N
100°08′19.6″E
@4410m a.s.l.

WCDA:
1 – 20 TeV
78,000m^2

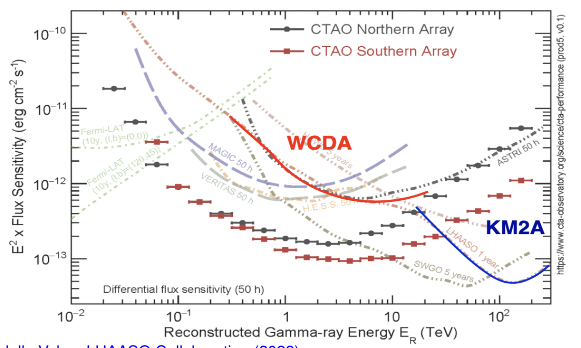

della Volpe, LHAASO Collaboration (2022)

WFCTA:
CR spec-trometer
> 10 TeV
18 tele-scopes

KM2A:
10 – 10^3 TeV
1188MDs
5612ED

LACT: array of 32 Air Cherenkov tele-scopes, is under construction now, and it will significantly improve the an-gular resolution and sensitivity as a

The First 12 Sources

The brightest UHE sources in the Galaxy

LHAASO 2021

Article

Extended Data Table 2 | List of energetic astrophysical objects possibly associated with each LHAASO source

LHAASO Source	Possible Origin	Type	Distance (kpc)	Age (kyr)[a]	L_s (erg/s)[b]	Potential TeV Counterpart[c]
LHAASO J0534+2202	PSR J0534+2200	PSR	2.0	1.26	4.5×10^{38}	Crab, Crab Nebula
LHAASO J1825-1326	PSR J1826-1334	PSR	3.1 ± 0.2[d]	21.4	2.8×10^{36}	HESS J1825-137, HESS J1826-130,
	PSR J1826-1256	PSR	1.6	14.4	3.6×10^{36}	2HWC J1825-134
LHAASO J1839-0545	PSR J1837-0604	PSR	4.8	33.8	2.0×10^{36}	2HWC J1837-065, HESS J1837-069,
	PSR J1838-0537	PSR	1.3[e]	4.9	6.0×10^{36}	HESS J1841-055
LHAASO J1843-0338	SNR G28.6-0.1	SNR	9.6 ± 0.3[f]	< 2[f]	—	HESS J1843-033, HESS J1844-030, 2HWC J1844-032
LHAASO J1849-0003	PSR J1849-0001	PSR	7[g]	43.1	9.8×10^{36}	HESS J1849-000, 2HWC J1849+001
	W43	YMC	5.5[h]	—	—	
LHAASO J1908+0621	SNR G40.5-0.5	SNR	3.4[i]	$\sim 10 - 20$[j]	—	MGRO J1908+06, HESS J1908+063,
	PSR 1907+0602	PSR	2.4	19.5	2.8×10^{36}	ARGO J1907+0627, VER J1907+062,
	PSR 1907+0631	PSR	3.4	11.3	5.3×10^{35}	2HWC 1908+063
LHAASO J1929+1745	PSR J1928+1746	PSR	4.6	82.6	1.6×10^{36}	2HWC J1928+177, 2HWC J1930+188,
	PSR J1930+1852	PSR	6.2	2.9	1.2×10^{37}	HESS J1930+188, VER J1930+188
	SNR G54.1+0.3	SNR	$6.3^{+0.8}_{-0.7}$[d]	$1.8 - 3.3$[k]	—	
LHAASO J1956+2845	PSR J1958+2846	PSR	2.0	21.7	3.4×10^{35}	2HWC J1955+285
	SNR G66.0-0.0	SNR	2.3 ± 0.2[d]	—	—	
LHAASO J2018+3651	PSR J2021+3651	PSR	$1.8^{+1.7}_{-1.4}$[l]	17.2	3.4×10^{36}	MGRO J2019+37, VER J2019+368,
	Sh 2-104	H II/YMC	3.3 ± 0.3[m]/4.0 ± 0.5[n]	—	—	VER J2016+371
LHAASO J2032+4102	Cygnus OB2	YMC	1.40 ± 0.08[o]	—	—	TeV J2032+4130, ARGO J2031+4157,
	PSR 2032+4127	PSR	1.40 ± 0.08[o]	201	1.5×10^{35}	MGRO J2031+41, 2HWC J2031+415,
	SNR G79.8+1.2	SNR candidate	—	—	—	VER J2032+414
LHAASO J2108+5157	—	—	—	—	—	—
LHAASO J2226+6057	SNR G106.3+2.7	SNR	0.8[p]	~ 10[p]	—	VER J2227+608, Boomerang Nebula
	PSR J2229+6114	PSR	0.8[p]	~ 10[p]	2.2×10^{37}	

The First 12 Sources

The brightest UHE sources in the Galaxy

LHAASO 2021

Article

Extended Data Table 2 | List of energetic astrophysical objects possibly associated with each LHAASO source

LHAASO Source	Possible Origin	Type	Distance (kpc)	Age (kyr)[a]	L_s (erg/s)[b]	Potential TeV Counterpart[c]
LHAASO J0534+2202	PSR J0534+2200	PSR	2.0	1.26	4.5×10^{38}	Crab, Crab Nebula
LHAASO J1825-1326	PSR J1826-1334	PSR	3.1 ± 0.2^d	21.4	2.8×10^{36}	HESS J1825-137, HESS J1826-130,
	PSR J1826-1256	PSR	1.6	14.4	3.6×10^{36}	2HWC J1825-134
LHAASO J1839-0545	PSR J1837-0604	PSR	4.8	33.8	2.0×10^{36}	2HWC J1837-065, HESS J1837-069,
	PSR J1838-0537	PSR	1.3^e	4.9	6.0×10^{36}	HESS J1841-055
LHAASO J1843-0338	SNR G28.6-0.1	SNR	9.6 ± 0.3^f	$< 2^f$	—	HESS J1843-033, HESS J1844-030,
						2HWC J1844-032
LHAASO J1849-0003	PSR J1849-0001	PSR	7^g	43.1	9.8×10^{36}	HESS J1849-000, 2HWC J1849+001
	W43	YMC	5.5^h	—	—	
LHAASO J1908+0621	SNR G40.5-0.5	SNR	3.4^i	$\sim 10 - 20^j$	—	MGRO J1908+06, HESS J1908+063,
	PSR 1907+0602	PSR	2.4	19.5	2.8×10^{36}	ARGO J1907+0627, VER J1907+062,
	PSR 1907+0631	PSR	3.4	11.3	5.3×10^{35}	2HWC 1908+063
LHAASO J1929+1745	PSR J1928+1746	PSR	4.6	82.6	1.6×10^{36}	2HWC J1928+177, 2HWC J1930+188,
	PSR J1930+1852	PSR	6.2	2.9	1.2×10^{37}	HESS J1930+188, VER J1930+188
	SNR G54.1+0.3	SNR	$6.3^{+0.8\ d}_{-0.7}$	$1.8 - 3.3^k$	—	
LHAASO J1956+2845	PSR J1958+2846	PSR	2.0	21.7	3.4×10^{35}	2HWC J1955+285
	SNR G66.0-0.0	SNR	2.3 ± 0.2^d	—	—	
LHAASO J2018+3651	PSR J2021+3651	PSR	$1.8^{+1.7\ l}_{-1.4}$	17.2	3.4×10^{36}	MGRO J2019+37, VER J2019+368,
	Sh 2-104	H II/YMC	$3.3 \pm 0.3^m/4.0 \pm 0.5^n$	—	—	VER J2016+371
LHAASO J2032+4102	Cygnus OB2	YMC	1.40 ± 0.08^o	—	—	TeV J2032+4130, ARGO J2031+4157,
	PSR 2032+4127	PSR	1.40 ± 0.08^o	201	1.5×10^{35}	MGRO J2031+41, 2HWC J2031+415,
	SNR G79.8+1.2	SNR candidate	—	—	—	VER J2032+414
LHAASO J2108+5157	—	—	—	—	—	—
LHAASO J2226+6057	SNR G106.3+2.7	SNR	0.8^p	$\sim 10^p$	—	VER J2227+608, Boomerang Nebula
	PSR J2229+6114	PSR	0.8^p	$\sim 10^p$	2.2×10^{37}	

The First LHAASO Catalogue

90 Sources & 43 UHE Sources

LHAASO 2024

1LHAASO Sources Associated Pulsars

Source Name	PSR Name	Sep. (deg)	d (kpc)	τ_c (kyr)	$\dot{E}$ (erg s^{-1})	P_c	Identified Type in TeVCat
1LHAASO J0007+7303u	PSR J0007+7303	0.05	1.40	14	4.5e+35	7.3e-05	PWN
1LHAASO J0216+4237u	PSR J0218+4232	0.33	3.15	476000	2.4e+35	3.6e-03	
1LHAASO J0249+6022	PSR J0248+6021	0.16	2.00	62	2.1e+35	1.5e-03	
1LHAASO J0359+5406	PSR J0359+5414	0.15	···	75	1.3e+36	7.2e-04	
1LHAASO J0534+2200u	PSR J0534+2200	0.01	2.00	1	4.5e+38	3.2e-06	PWN
1LHAASO J0542+2311u	PSR J0543+2329	0.30	1.56	253	4.1e+34	8.3e-03	
1LHAASO J0622+3754	PSR J0622+3749	0.09	···	208	2.7e+34	2.5e-04	PWN/TeV Halo
1LHAASO J0631+1040	PSR J0631+1037	0.11	2.10	44	1.7e+35	3.5e-04	PWN
1LHAASO J0634+1741u	PSR J0633+1746	0.12	0.19	342	3.3e+34	1.3e-03	PWN/TeV Halo
1LHAASO J0635+0619	PSR J0633+0632	0.39	1.35	59	1.2e+35	9.4e-03	
1LHAASO J1740+0948u	PSR J1740+1000	0.21	1.23	114	2.3e+35	1.4e-03	
1LHAASO J1809-1918u	PSR J1809-1917	0.05	3.27	51	1.8e+36	6.2e-04	
1LHAASO J1813-1245	PSR J1813-1245	0.01	2.63	43	6.2e+36	6.3e-06	
1LHAASO J1825-1256u	PSR J1826-1256	0.09	1.55	14	3.6e+36	1.6e-03	
1LHAASO J1825-1337u	PSR J1826-1334	0.11	3.61	21	2.8e+36	2.8e-03	PWN/TeV Halo
1LHAASO J1837-0654u	PSR J1838-0655	0.12	6.60	23	5.6e+36	2.2e-03	PWN
1LHAASO J1839-0548u	PSR J1838-0537	0.20	···	5	6.0e+36	6.1e-03	
1LHAASO J1848-0001u	PSR J1849-0001	0.06	···	43	9.8e+36	1.2e-04	PWN
1LHAASO J1857+0245	PSR J1856+0245	0.16	6.32	21	4.6e+36	3.1e-03	PWN
1LHAASO J1906+0712	PSR J1906+0722	0.19	···	49	1.0e+36	5.9e-03	
1LHAASO J1908+0615u	PSR J1907+0602	0.23	2.37	20	2.8e+36	6.8e-03	
1LHAASO J1912+1014u	PSR J1913+1011	0.13	4.61	169	2.9e+36	1.5e-03	
1LHAASO J1914+1150u	PSR J1915+1150	0.09	14.01	116	5.4e+35	1.8e-03	
1LHAASO J1928+1746u	PSR J1928+1746	0.04	4.34	83	1.6e+36	1.6e-04	
1LHAASO J1929+1846u	PSR J1930+1852	0.29	7.00	3	1.2e+37	2.6e-03	PWN
1LHAASO J1954+2836u	PSR J1954+2836	0.01	1.96	69	1.1e+36	1.6e-05	PWN
1LHAASO J1954+3253	PSR J1952+3252	0.33	3.00	107	3.7e+36	6.7e-03	
1LHAASO J1959+2846u	PSR J1958+2845	0.10	1.95	22	3.4e+35	2.8e-03	PWN
1LHAASO J2005+3415	PSR J2004+3429	0.25	10.78	18	5.8e+35	9.9e-03	
1LHAASO J2005+3050	PSR J2006+3102	0.20	6.04	104	2.2e+35	9.2e-03	
1LHAASO J2020+3649u	PSR J2021+3651	0.05	1.80	17	3.4e+36	1.5e-04	PWN
1LHAASO J2028+3352	PSR J2028+3332	0.36	···	576	3.5e+34	8.0e-03	
1LHAASO J2031+4127u	PSR J2032+4127	0.08	1.33	201	1.5e+35	1.0e-03	PWN
1LHAASO J2228+6100u	PSR J2229+6114	0.27	3.00	10	2.2e+37	2.2e-03	PWN
1LHAASO J2238+5900	PSR J2238+5903	0.07	2.83	27	8.9e+35	3.0e-04	

35 sources in 1LHAASO are linked to PRSs

The First LHAASO Catalogue

90 Sources & 43 UHE Sources

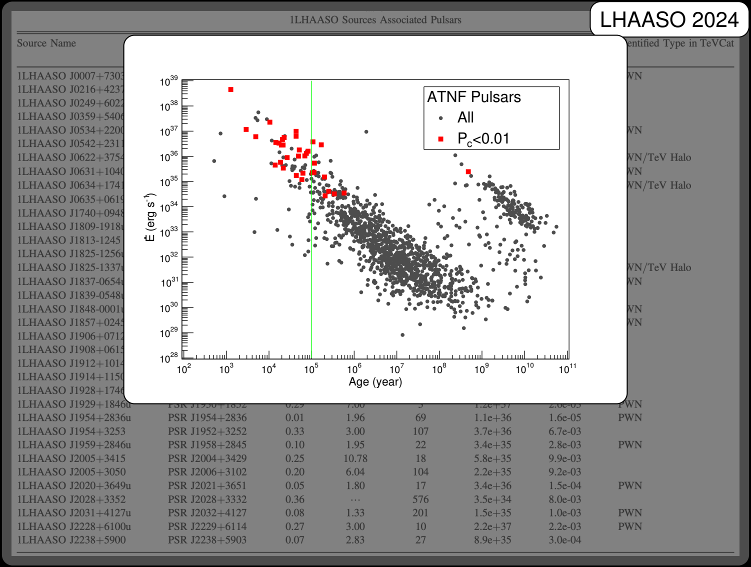
1LHAASO Sources Associated Pulsars

Source Name							entified Type in TeVCat
1LHAASO J0007+7303							WN
1LHAASO J0216+4237							
1LHAASO J0249+6022							
1LHAASO J0359+5406							
1LHAASO J0534+2200							WN
1LHAASO J0542+2311							
1LHAASO J0622+3754							WN/TeV Halo
1LHAASO J0631+1040							WN
1LHAASO J0634+1741							WN/TeV Halo
1LHAASO J0635+0619							
1LHAASO J1740+0948							
1LHAASO J1809-1918u							
1LHAASO J1813-1245							
1LHAASO J1825-1256u							
1LHAASO J1825-1337u							WN/TeV Halo
1LHAASO J1837-0654u							WN
1LHAASO J1839-0548u							
1LHAASO J1848-0001u							WN
1LHAASO J1857+0245							WN
1LHAASO J1906+0712							
1LHAASO J1908+0615							
1LHAASO J1912+1014							
1LHAASO J1914+1150							
1LHAASO J1928+1746							
1LHAASO J1929+1846u	PSR J1930+1852	0.29	7.00	5	1.2e+37	2.6e-05	PWN
1LHAASO J1954+2836u	PSR J1954+2836	0.01	1.96	69	1.1e+36	1.6e-05	PWN
1LHAASO J1954+3253	PSR J1952+3252	0.33	3.00	107	3.7e+36	6.7e-03	
1LHAASO J1959+2846u	PSR J1958+2845	0.10	1.95	22	3.4e+35	2.8e-03	PWN
1LHAASO J2005+3415	PSR J2004+3429	0.25	10.78	18	5.8e+35	9.9e-03	
1LHAASO J2005+3050	PSR J2006+3102	0.20	6.04	104	2.2e+35	9.2e-03	
1LHAASO J2020+3649u	PSR J2021+3651	0.05	1.80	17	3.4e+36	1.5e-04	PWN
1LHAASO J2028+3352	PSR J2028+3332	0.36	⋯	576	3.5e+34	8.0e-03	
1LHAASO J2031+4127u	PSR J2032+4127	0.08	1.33	201	1.5e+35	1.0e-03	PWN
1LHAASO J2228+6100u	PSR J2229+6114	0.27	3.00	10	2.2e+37	2.2e-03	PWN
1LHAASO J2238+5900	PSR J2238+5903	0.07	2.83	27	8.9e+35	3.0e-04	

LHAASO 2024

The First LHAASO Catalogue

90 Sources & 43 UHE Sources

LHAASO 2024

1LHAASO Sources Associated Pulsars

Source Name							Identified Type in TeVCat
1LHAASO J0007+7303							WN
1LHAASO J0216+4237							
1LHAASO J0249+6022							
1LHAASO J0359+5406							
1LHAASO J0534+2200							
1LHAASO J0542+2311							
1LHAASO J0622+3754							
1LHAASO J0631+1040							
1LHAASO J0634+1741							
1LHAASO J0635+0619							
1LHAASO J1740+0948							
1LHAASO J1809-1918u							
1LHAASO J1813-1245							
1LHAASO J1825-1256u							
1LHAASO J1825-1337u							
1LHAASO J1837-0654u							
1LHAASO J1839-0548u							
1LHAASO J1848-0001u							
1LHAASO J1857+0245							WN
1LHAASO J1906+0712							
1LHAASO J1908+0615							
1LHAASO J1912+1014							
1LHAASO J1914+1150							
1LHAASO J1928+1746							
1LHAASO J1929+1846u	PSR J1930+1852	0.29	7.00	5	1.2e+37	2.6e-05	PWN
1LHAASO J1954+2836u	PSR J1954+2836	0.01	1.96	69	1.1e+36	1.6e-05	PWN
1LHAASO J1954+3253	PSR J1952+3252	0.33	3.00	107	3.7e+36	6.7e-03	
1LHAASO J1959+2846u	PSR J1958+2845	0.10	1.95	22	3.4e+35	2.8e-03	PWN
1LHAASO J2005+3415	PSR J2004+3429	0.25	10.78	18	5.8e+35	9.9e-03	
1LHAASO J2005+3050	PSR J2006+3102	0.20	6.04	104	2.2e+35	9.2e-03	
1LHAASO J2020+3649u	PSR J2021+3651	0.05	1.80	17	3.4e+36	1.5e-04	PWN
1LHAASO J2028+3352	PSR J2028+3332	0.36	…	576	3.5e+34	8.0e-03	
1LHAASO J2031+4127u	PSR J2032+4127	0.08	1.33	201	1.5e+35	1.0e-03	PWN
1LHAASO J2228+6100u	PSR J2229+6114	0.27	3.00	10	2.2e+37	2.2e-03	PWN
1LHAASO J2238+5900	PSR J2238+5903	0.07	2.83	27	8.9e+35	3.0e-04	

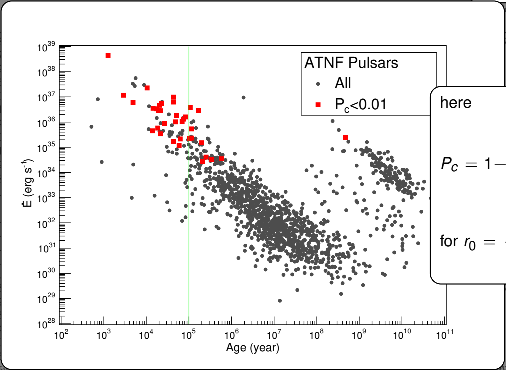

here

$$P_c = 1 - \exp\left[-\frac{r^2}{r_0^2}\right]$$

$$\text{for } r_0 = \frac{1}{\sqrt{\pi\rho(\dot{E})}}$$

Fundamental Constraints on Leptonic PeVatrons

Short Cooling Time

- ☞ Leptons lose energy very easily
  $t_{\rm syn} \approx 5 \times 10^2 \left(\frac{B}{5\,\mu\rm G}\right)^{-2} \left(\frac{E}{1\,\rm PeV}\right)^{-1} \rm yr$
- ☞ This implies a limited propagation length (here $D = D_0(E/1\,\rm PeV)^\delta$)

$$R_{\rm dif} \approx 10^2 {\rm pc} \times \frac{\left(\frac{D_0}{10^{30}\,\frac{\rm cm^2}{\rm s}}\right)^{\frac{1}{2}}}{\left(\frac{B}{5\,\mu\rm G}\right)\left(\frac{E}{1\rm PeV}\right)^{\frac{1-\delta}{2}}}$$

Klein-Nishina Cutoff

Inverse Compton scattering dominates the production of γ rays by electrons in VHE and UHE regimes

- ☞ In the Thomson regime, electrons radiates away only a small fraction of its energy, $\epsilon\omega/(m_e^2 c^4)$ [$\ll 1$]
- ☞ In the Klein-Nishina regime, the cross section decreases considerably, so the efficiency of the process drops

Hillas Criterion

Source Size, $R > R_{\mathcal{G}} = 10^{18}\left(\frac{B}{5\mu\rm G}\right)^{-1}\left(\frac{E}{1\rm PeV}\right)\rm cm$, and electric potential drop, $\epsilon_{\rm max} < e\Delta\Phi$, limits the maximum energy of accelerated particles

Short Cooling Time / Transport

- Galactic sources are relatively small:

$$\frac{R}{d} \sim 0.2^\circ \frac{(R/10\mathrm{pc})}{(d/3\mathrm{kpc})}$$

i.e., likely all extended sources seen by LHAASO include the source and its vicinity

- High-energy electrons must met different environmental conditions, on their way across these scales
- The length scale defined by observation may cover several physical scales, and the dominant transport scenario can change accordingly
- Furthermore, on a sub-degree scale the transport can be very complex falling in the middle of the standard approximations ("not yet diffusion")

- Blast Wave Radius

$$R \approx 20\mathrm{pc} \times \frac{\left(\frac{E}{10^{50}\mathrm{erg}}\right)^{1/5}\left(\frac{t}{10^{5}\mathrm{yr}}\right)^{2/5}}{\frac{n}{1\mathrm{cm}^{-3}}}$$

Short Cooling Time / Transport

- Galactic sources are relatively small:

$$\frac{R}{d} \sim 0.2^\circ \frac{(R/10\mathrm{pc})}{(d/3\mathrm{kpc})}$$

  i.e., likely all extended sources seen by LHAASO include the source and its vicinity

- High-energy electrons must met different environmental conditions, on their way across these scales
- The length scale defined by observation may cover several physical scales, and the dominant transport scenario can change accordingly
- Furthermore, on a sub-degree scale the transport can be very complex falling in the middle of the standard approximations ("not yet diffusion")

- Blast Wave Radius

$$R \approx 20\mathrm{pc} \times \frac{\left(\frac{E}{10^{50}\mathrm{erg}}\right)^{1/5}\left(\frac{t}{10^5\mathrm{yr}}\right)^{2/5}}{\frac{n}{1\mathrm{cm}^{-3}}}$$

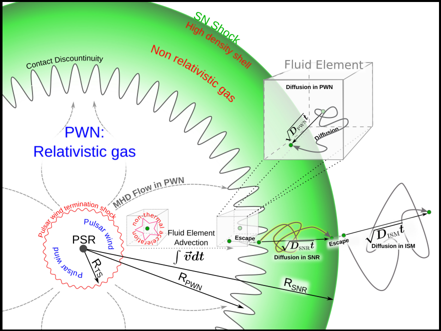

Short Cooling Time / Transport

- Galactic sources are relatively small:

$$\frac{R}{d} \sim 0.2^\circ \frac{(R/10\mathrm{pc})}{(d/3\mathrm{kpc})}$$

i.e., likely all extended sources seen by LHAASO include the source and its vicinity

- High-energy electrons must met different environmental conditions, on their way across these scales
- The length scale defined by observation may cover several physical scales, and the dominant transport scenario can change accordingly
- Furthermore, on a sub-degree scale the transport can be very complex falling in the middle of the standard approximations ("not yet diffusion")

- Blast Wave Radius

$$R \approx 20\mathrm{pc} \times \frac{\left(\frac{E}{10^{50}\mathrm{erg}}\right)^{1/5}\left(\frac{t}{10^5\mathrm{yr}}\right)^{2/5}}{\frac{n}{1\mathrm{cm}^{-3}}}$$

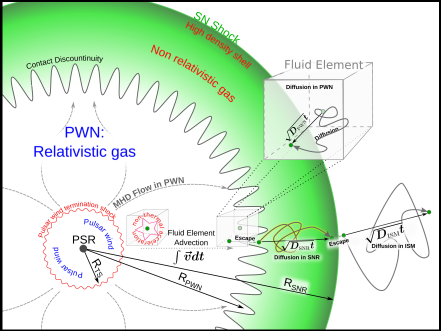

Short Cooling Time / Transport

- Galactic sources are relatively small:

$$\frac{R}{d} \sim 0.2^{\circ} \frac{(R/10\mathrm{pc})}{(d/3\mathrm{kpc})}$$

i.e., likely all extended sources seen by LHAASO include the source and its vicinity

- High-energy electrons must met different environmental conditions, on their way across these scales

- The length scale defined by observation may cover several physical scales, and the dominant transport scenario can change accordingly

- Furthermore, on a sub-degree scale the transport can be very complex falling in the middle of the standard approximations (“not yet diffusion”)

- Blast Wave Radius

$$R \approx 20\mathrm{pc} \times \frac{\left(\frac{E}{10^{50}\mathrm{erg}}\right)^{1/5}\left(\frac{t}{10^{5}\mathrm{yr}}\right)^{2/5}}{\frac{n}{1\mathrm{cm}^{-3}}}$$

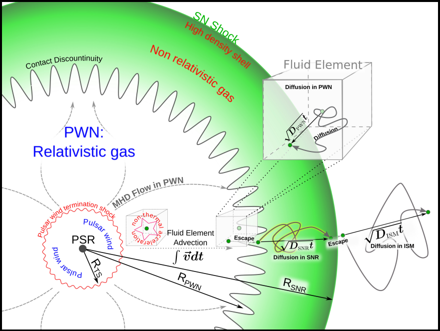

- Diffusion speed, $R_{\rm dif}/t$

$$\frac{v_{\rm dif}}{c} = \frac{6D}{Rc} \approx 1.3 \frac{\frac{D}{10^{30}\,\frac{\mathrm{cm}^2}{\mathrm{s}}}}{\frac{R}{50\mathrm{pc}}}$$

Klein-Nishina Cutoff

☞ A high-energy electrons up-scatters a low-energy photon:

$$p_0 + k_0 \to p_1 + k_1$$

in the electron rest frame the the incident photon energy is

$$\omega' = \frac{(p_0 k_0)}{m_e}$$

☞ In the regime when $\omega' \gtrsim m_e c^2$, the electron recoil needs to be accounted for, i.e., the cross-section starts to deviate from the classical (Thomson value) when

$$\omega\epsilon \sim m_e^2 c^4 \to \epsilon \sim 0.3\mathrm{TeV}\left(\frac{\omega}{1\mathrm{eV}}\right)^{-1}$$

☞ Cross-section obtained with QED features a significant reduction in high-energy regime (the Klein-Nishina effect)

Klein-Nishina Cutoff

- A high-energy electrons up-scatters a low-energy photon:

$$p_0 + k_0 \to p_1 + k_1$$

in the electron rest frame the the incident photon energy is

$$\omega' = \frac{(p_0 k_0)}{m_e}$$

- In the regime when $\omega' \gtrsim m_e c^2$, the electron recoil needs to be accounted for, i.e., the cross-section starts to deviate from the classical (Thomson value) when

$$\omega\epsilon \sim m_e^2 c^4 \to \epsilon \sim 0.3\mathrm{TeV}\left(\frac{\omega}{1\mathrm{eV}}\right)^{-1}$$

- Cross-section obtained with QED features a significant reduction in high-energy regime (the Klein-Nishina effect)

Klein-Nishina Cutoff

- A high-energy electrons up-scatters a low-energy photon:

$$p_0 + k_0 \to p_1 + k_1$$

  in the electron rest frame the the incident photon energy is

$$\omega' = \frac{(p_0 k_0)}{m_e}$$

- In the regime when $\omega' \gtrsim m_e c^2$, the electron recoil needs to be accounted for, i.e., the cross-section starts to deviate from the classical (Thomson value) when

$$\omega\epsilon \sim m_e^2 c^4 \to \epsilon \sim 0.3\mathrm{TeV}\left(\frac{\omega}{1\mathrm{eV}}\right)^{-1}$$

- Cross-section obtained with QED features a significant reduction in high-energy regime (the Klein-Nishina effect)

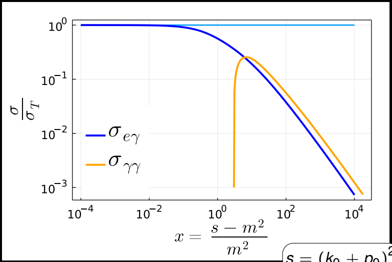

$s = (k_0 + p_0)^2$

Klein-Nishina Cutoff

- A high-energy electrons up-scatters a low-energy photon:

$$p_0 + k_0 \to p_1 + k_1$$

in the electron rest frame the the incident photon energy is

$$\omega' = \frac{(p_0 k_0)}{m_e}$$

- In the regime when $\omega' \gtrsim m_e c^2$, the electron recoil needs to be accounted for, i.e., the cross-section starts to deviate from the classical (Thomson value) when

$$\omega\epsilon \sim m_e^2 c^4 \to \epsilon \sim 0.3\mathrm{TeV}\left(\frac{\omega}{1\mathrm{eV}}\right)^{-1}$$

- Cross-section obtained with QED features a significant reduction in high-energy regime (the Klein-Nishina effect)

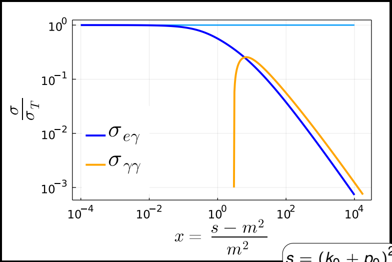

$s = (k_0 + p_0)^2$

- What is the lowest energy of low-energy target?

$$\omega \approx 3kT\Big|_{T=2.7^\circ\mathrm{K}} \approx 10^{-3}\ \mathrm{eV}$$

- Thus, the Klein-Nishina cutoff is important for

$$\epsilon \gtrsim 400\mathrm{TeV}$$

i.e., in all UHE sources

CMBR & UHE Sources

If one measures a γ-ray spectrum with LHAASO from a PeVatron. Can one determine its nature (leptonic vs hadronic) based just on the spectral properties using the Klein-Nishina effect?

CMBR & UHE Sources

If one measures a γ-ray spectrum with LHAASO from a PeVatron. Can one determine its nature (leptonic vs hadronic) based just on the spectral properties using the Klein-Nishina effect?

- ☞ CMBR provides the dominant target for production of the PeV emission
- ☞ Of course, CMBR photons are up-scattered to differnt energies by different electrons

$$\epsilon \approx \frac{m_e^2 c^4}{4\omega} \frac{v^{1/2}\left(1+2v^{1/2}\right)}{2} \sqrt{\frac{\ln\left(1+v^{1/2}\right)}{\ln\left(1+v^{1/2}/3\right)}}$$

where ϵ, ε are electron/photon energies, and $v = \frac{4\varepsilon k_B T}{m_e^2 c^4} \approx 3.5 \frac{\varepsilon}{1\mathrm{PeV}} \frac{T}{2.7\mathrm{K}}$

- ☞ Does an "almost power-law" spectrum rules out the leptonic scenario?

CMBR & UHE Sources

If one measures a γ-ray spectrum with LHAASO from a PeVatron. Can one determine its nature (leptonic vs hadronic) based just on the spectral properties using the Klein-Nishina effect?

- CMBR provides the dominant target for production of the PeV emission
- Of course, CMBR photons are up-scattered to differnt energies by different electrons

$$\epsilon \approx \frac{m_e^2 c^4}{4\omega} \frac{v^{1/2}\left(1 + 2v^{1/2}\right)}{2} \sqrt{\frac{\ln\left(1 + v^{1/2}\right)}{\ln\left(1 + v^{1/2}/3\right)}}$$

where ϵ, ε are electron/photon energies, and $v = \frac{4\varepsilon k_B T}{m_e^2 c^4} \approx 3.5 \frac{\varepsilon}{1\mathrm{PeV}} \frac{T}{2.7\mathrm{K}}$

- Does an "almost power-law" spectrum rules out the leptonic scenario?

CMBR & UHE Sources

If one measures a γ-ray spectrum with LHAASO from a PeVatron. Can one determine its nature (leptonic vs hadronic) based just on the spectral properties using the Klein-Nishina effect?

- ☞ CMBR provides the dominant target for production of the PeV emission
- ☞ Of course, CMBR photons are up-scattered to differnt energies by different electrons

$$\epsilon \approx \frac{m_e^2 c^4}{4\omega} \frac{v^{1/2}\left(1+2v^{1/2}\right)}{2} \sqrt{\frac{\ln\left(1+v^{1/2}\right)}{\ln\left(1+v^{1/2}/3\right)}}$$

where ϵ, ε are electron/photon energies, and $v = \frac{4\varepsilon k_B T}{m_e^2 c^4} \approx 3.5 \frac{\varepsilon}{1\mathrm{PeV}} \frac{T}{2.7\mathrm{K}}$

- ☞ Does an "almost power-law" spectrum rules out the leptonic scenario?

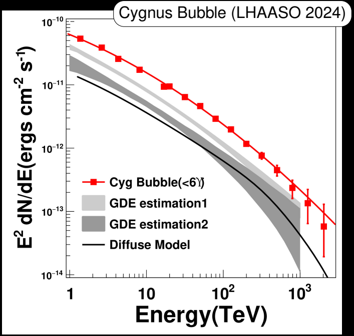

- ☞ The 1–30 TeV range defines the power-law slope
- ☞ The 30 – 10^3 TeV range requires an implausible high-energy cutoff (or even hardening) to compensate for the Klein-Nishina cutoff

Fitting Cygnus Bubble with IC

Let's fit the spectrum with an inverse Compton model using `naima` by V.Zabalza

Naima is a Python package for computation of non-thermal radiation from relativistic particle populations. It includes tools to perform MCMC fitting of radiative models to X-ray, GeV, and TeV spectra using emcee, an affine-invariant ensemble sampler for Markov Chain Monte Carlo. Naima is an Astropy affiliated package.

There are two main components of the package: a set of nonthermal Radiative Models, and a set of utility functions that make it easier to fit a given model to observed spectral data (see Model fitting).

Nonthermal radiative models are available for Synchrotron, inverse Compton, Bremsstrahlung, and neutral pion decay processes. All of the models allow the use of an arbitrary shape of the particle energy distribution, and several functional models are also available to be used as particle distribution functions. See Radiative Models for a detailed explanation of these.

from https://naima.readthedocs.io/en/latest/

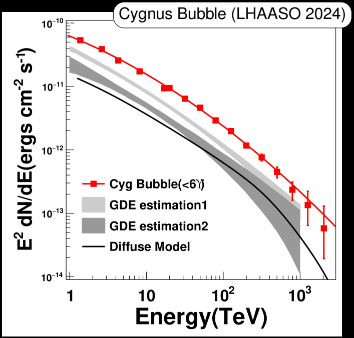

Fitting Cygnus Bubble with IC

Let's fit the spectrum with an inverse Compton model using `naima` by V.Zabalza

- The most basic model ECPL with flat posterior distributions $\frac{dN}{d\epsilon} = A\left(\frac{\epsilon}{\epsilon_0}\right)^{-\alpha} \exp\left[-\left(\frac{\epsilon}{\epsilon_c}\right)\right]$ up-scatter CMBR
- The most basic model ECPL with a non-flat posterior distributions for cutoff energy $\frac{dN}{d\epsilon} = A\left(\frac{\epsilon}{\epsilon_0}\right)^{-\alpha} \exp\left[-\left(\frac{\epsilon}{\epsilon_c}\right)\right]$ up-scatter CMBR
- In fact, even the simplest model should be more complicated: $\frac{dN}{d\epsilon} = A\left(\frac{\epsilon}{\epsilon_0}\right)^{-\alpha} \exp\left[-\left(\frac{\epsilon}{\epsilon_c}\right)\right]$ up-scatter CMBR and some higher-temperature photon fields

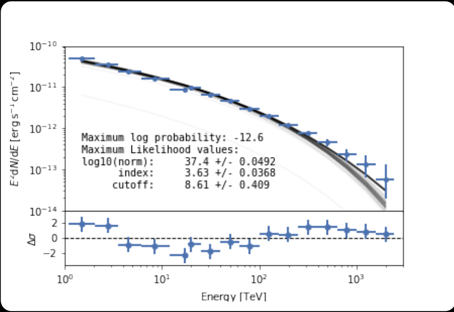

- Exponential cutoff in electron spectrum appears at $\approx$ 10PeV
- Power-law index is quite steep$\approx$ 3.6

Fitting Cygnus Bubble with IC

Let's fit the spectrum with an inverse Compton model using `naima` by V.Zabalza

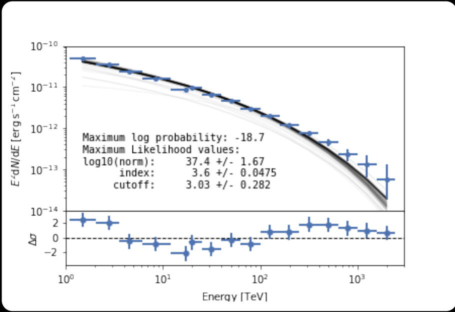

- ☞ The most basic model ECPL with flat posterior distributions
$$\frac{\mathrm{d}N}{\mathrm{d}\epsilon} = A\left(\frac{\epsilon}{\epsilon_0}\right)^{-\alpha} \exp\left[-\left(\frac{\epsilon}{\epsilon_c}\right)\right]$$
up-scatter CMBR
- ☞ The most basic model ECPL with a non-flat posterior distributions for cutoff energy
$$\frac{\mathrm{d}N}{\mathrm{d}\epsilon} = A\left(\frac{\epsilon}{\epsilon_0}\right)^{-\alpha} \exp\left[-\left(\frac{\epsilon}{\epsilon_c}\right)\right]$$
up-scatter CMBR
- ☞ In fact, even the simplest model should be more complicated:
$$\frac{\mathrm{d}N}{\mathrm{d}\epsilon} = A\left(\frac{\epsilon}{\epsilon_0}\right)^{-\alpha} \exp\left[-\left(\frac{\epsilon}{\epsilon_c}\right)\right]$$
up-scatter CMBR and some higher-temperature photon fields

- ☞ Exponential cutoff in electron spectrum shifts to $\approx$ 3PeV
- ☞ Power-law index remains unchanged$\approx$ 3.6

Fitting Cygnus Bubble with IC

Let's fit the spectrum with an inverse Compton model using `naima` by V.Zabalza

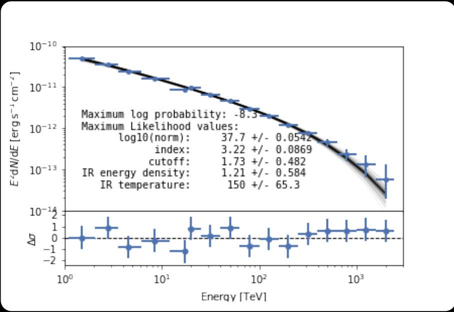

- The most basic model ECPL with flat posterior distributions $$\frac{dN}{d\epsilon} = A\left(\frac{\epsilon}{\epsilon_0}\right)^{-\alpha}\exp\left[-\left(\frac{\epsilon}{\epsilon_c}\right)\right]$$ up-scatter CMBR
- The most basic model ECPL with a non-flat posterior distributions for cutoff energy $$\frac{dN}{d\epsilon} = A\left(\frac{\epsilon}{\epsilon_0}\right)^{-\alpha}\exp\left[-\left(\frac{\epsilon}{\epsilon_c}\right)\right]$$ up-scatter CMBR
- In fact, even the simplest model should be more complicated: $$\frac{dN}{d\epsilon} = A\left(\frac{\epsilon}{\epsilon_0}\right)^{-\alpha}\exp\left[-\left(\frac{\epsilon}{\epsilon_c}\right)\right]$$ up-scatter CMBR and some higher-temperature photon fields

- Exponential cutoff in electron spectrum shifts to the values smaller that the highest energy γ-ray point, to ≈ 1.7PeV
- Power-law index is getting noticeably harder ≈ 3.2
- The properties of IR photon field are quite reasonable

Hillas Criterion

$$R > R_{\mathcal{G}} = \frac{\epsilon_{\max}}{eB} \Rightarrow \epsilon_{\max} < eBR \approx 5\mathrm{PeV}\frac{B}{5\mu\mathrm{G}}\frac{R}{1\mathrm{pc}}$$

Hillas Criterion

$$R > R_{\mathcal{G}} = \frac{\epsilon_{\max}}{eB} \Rightarrow \epsilon_{\max} < eBR \approx 5\mathrm{PeV}\frac{B}{5\mu\mathrm{G}}\frac{R}{1\mathrm{pc}}$$

Potential drop

- Electric field is $\mathcal{E} = \frac{v_{\mathrm{blk}}}{c} B$
- Potential drop $\Delta\Phi_{\max} = \frac{v_{\mathrm{blk}}}{c} BR$
- Maximum energy $\epsilon_{\max} < \frac{v_{\mathrm{blk}}}{c} eBR$

Hillas Criterion

$$R > R_{\mathcal{G}} = \frac{\epsilon_{\rm max}}{eB} \Rightarrow \epsilon_{\rm max} < eBR \approx 5\mathrm{PeV}\frac{B}{5\mu\mathrm{G}}\frac{R}{1\mathrm{pc}}$$

Potential drop

- Electric field is $\mathcal{E} = \frac{v_{\rm blk}}{c}B$
- Potential drop $\Delta\Phi_{\rm max} = \frac{v_{\rm blk}}{c}BR$
- Maximum energy $\epsilon_{\rm max} < \frac{v_{\rm blk}}{c}eBR$

Acceleration-Losses Balance

- Accelerating Electric field is $\mathcal{E}_{\rm ac} = B/\eta$
- Synchrotron losses $t_{\rm syn} = -\epsilon/\dot{\epsilon}$
- Maximum energy, $\dot{\epsilon} < ec\mathcal{E}_{\rm ac}$:

$$t_{\rm syn} > \frac{\eta\epsilon_{\rm max}}{ceB} \rightarrow \epsilon_{\rm max} < \left(\frac{t_{\rm syn}}{cR\eta}\right)eBR$$

$$\epsilon_{\rm max} < 30\mathrm{PeV}\eta^{-1/2}\left(\frac{B}{5\mu\mathrm{G}}\right)^{-1/2}$$

Hillas Criterion

$$R > R_{\mathcal{G}} = \frac{\epsilon_{\max}}{eB} \Rightarrow \epsilon_{\max} < eBR \approx 5\mathrm{PeV}\frac{B}{5\mu\mathrm{G}}\frac{R}{1\mathrm{pc}}$$

Potential drop

- Electric field is $\mathcal{E} = \frac{v_{\mathrm{blk}}}{c}B$
- Potential drop $\Delta\Phi_{\max} = \frac{v_{\mathrm{blk}}}{c}BR$
- Maximum energy $\epsilon_{\max} < \frac{v_{\mathrm{blk}}}{c}eBR$

Acceleration-Losses Balance

- Accelerating Electric field is $\mathcal{E}_{\mathrm{ac}} = B/\eta$
- Synchrotron losses $t_{\mathrm{syn}} = -\epsilon/\dot{\epsilon}$
- Maximum energy, $\dot{\epsilon} < ec\mathcal{E}_{\mathrm{ac}}$:

$$t_{\mathrm{syn}} > \frac{\eta\epsilon_{\max}}{ceB} \to \epsilon_{\max} < \left(\frac{t_{\mathrm{syn}}}{cR\eta}\right)eBR$$

$$\epsilon_{\max} < 30\mathrm{PeV}\eta^{-1/2}\left(\frac{B}{5\mu\mathrm{G}}\right)^{-1/2}$$

Another formulation: energy flux from the source

$$\frac{\beta cB^2}{4\pi} = \frac{\sigma L}{(4\pi R^2\Delta\Omega)} \Rightarrow BR = \sqrt{\frac{\sigma}{\beta\Delta\Omega}}\sqrt{\frac{L}{c}}$$

$$\epsilon_{\max} < \sqrt{\frac{\sigma\beta}{\Delta\Omega}}\sqrt{\frac{Le^2}{c}}$$

outflow parameter:

- σ is magenetization
- β is bulk speed
- $\Delta\Omega$ is outflow solid angle

Hillas Criterion

$$\epsilon_{\rm max} < \sqrt{\frac{\sigma\beta}{\Delta\Omega}}\sqrt{\frac{Le^2}{c}} \approx 20\,{\rm PeV}\sqrt{\frac{\sigma\beta}{\Delta\Omega}}\sqrt{\frac{L}{10^{38}\,\frac{\rm erg}{\rm s}}}$$

Hillas Criterion

$$\epsilon_{\max} < \sqrt{\frac{\sigma\beta}{\Delta\Omega}}\sqrt{\frac{Le^2}{c}} \approx 20\mathrm{PeV}\sqrt{\frac{\sigma\beta}{\Delta\Omega}}\sqrt{\frac{L}{10^{38}\,\frac{\mathrm{erg}}{\mathrm{s}}}}$$

- ? How strongly can the parameters in this estimate vary?
- ☞ The solid angle of the outflow, $\Delta\Omega$, for Galactic sources should be large (with exclusion of μQs?)
- ☞ Bulk speed, β, may ranger from $\beta = 1$ for pulsar winds to $\beta \sim 10^{-2}$ for stellar wind
- ☞ Outflow magnetization, σ, is probably small between 10^{-2} and 10^{-6}

Hillas Criterion

$$\epsilon_{\rm max} < \sqrt{\frac{\sigma\beta}{\Delta\Omega}}\sqrt{\frac{Le^2}{c}} \approx 20{\rm PeV}\sqrt{\frac{\sigma\beta}{\Delta\Omega}}\sqrt{\frac{L}{10^{38}\frac{\rm erg}{\rm s}}}$$

- **?** How strongly can the parameters in this estimate vary?
- ☞ The solid angle of the outflow, $\Delta\Omega$, for Galactic sources should be large (with exclusion of μQs?)
- ☞ Bulk speed, β, may ranger from $\beta = 1$ for pulsar winds to $\beta \sim 10^{-2}$ for stellar wind
- ☞ Outflow magnetization, σ, is probably small between 10^{-2} and 10^{-6}

Promising sources

- ☞ SN shocks (DSA): $\beta = 3 \cdot 10^{-2}, \sigma \sim 10^{-6}, \Delta\Omega \sim 1$
- ☞ Stellar clusters (DSA): $\beta = 5 \cdot 10^{-3}, \sigma \sim 5 \cdot 10^{-5}, \Delta\Omega \sim 1$
- ☞ Pulsar wind termination shocks (rel): $\beta = 1, \sigma \sim 10^{-2}, \Delta\Omega \sim 1$ and $L \sim 10^{37}\frac{\rm erg}{\rm s}$ (no protons!)
- ☞ μQs (DSA): $\beta \sim 0.1, \sigma \sim 10^{-2}, \Delta\Omega \sim 0.1$ and $L \sim 10^{39}\frac{\rm erg}{\rm s}$

Pulsar Magnetosphere

Two important length scales:

$$R_{\rm lc} = \frac{c}{\Omega} \approx 10^3 \mathrm{km}$$

$$R_{\rm pc} = R_{\rm psr}\sqrt{\frac{\Omega R_{\rm psr}}{c}} \approx 0.1 \mathrm{km}$$

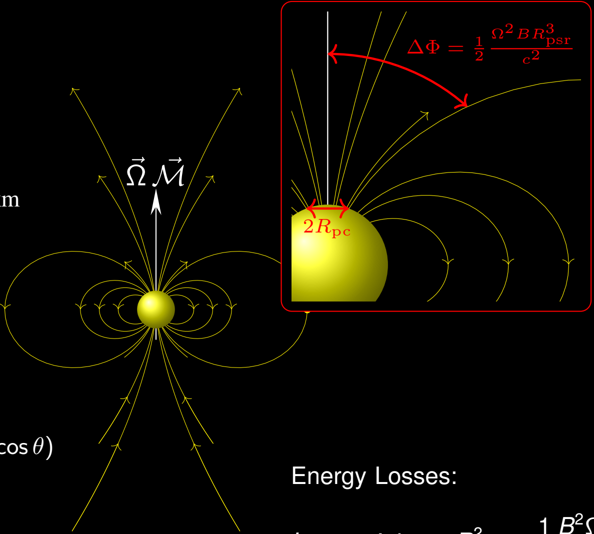

Electric potential (vacuum):

$$\Phi(r,\theta) = \frac{1}{3}\frac{\Omega B R^5}{c} r^{-3}\mathcal{P}_2(\cos\theta)$$

Plasma charge density:

$$\rho_{\rm GJ} = \frac{\Omega B}{2\pi c}$$

(Goldreich-Julian density)

Pulsars are very efficient plasma “machines”

Energy Losses:

$$L_{\rm wind} \approx \Delta\Phi \rho_{\rm GJ} \pi R_{\rm pc}^2 c \sim \frac{1}{4}\frac{B^2\Omega^4 R^6}{c^3}$$

$$L_{\rm sd} = I\Omega\dot{\Omega} \sim \frac{1}{6}\frac{B^2\Omega^4 R^6}{c^3}$$

Pulsar Magnetosphere

Arons 1997

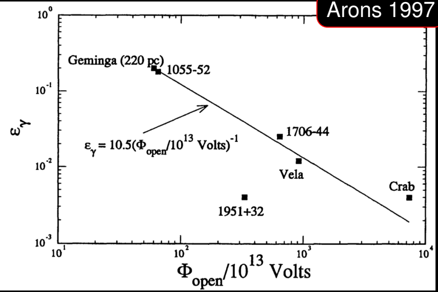

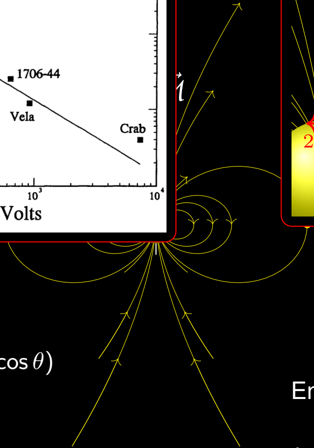

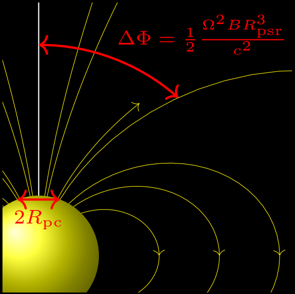

Electric potential (vacuum):

$$\Phi(r,\theta) = \frac{1}{3}\frac{\Omega B R^5}{c} r^{-3}\mathcal{P}_2(\cos\theta)$$

Plasma charge density:

$$\rho_{\rm GJ} = \frac{\Omega B}{2\pi c}$$

(Goldreich-Julian density)

Pulsars are very efficient plasma “machines”

Energy Losses:

$$L_{\rm wind} \approx \Delta\Phi \rho_{\rm GJ}\pi R_{\rm pc}^2 c \sim \frac{1}{4}\frac{B^2\Omega^4 R^6}{c^3}$$

$$L_{\rm sd} = I\Omega\dot{\Omega} \sim \frac{1}{6}\frac{B^2\Omega^4 R^6}{c^3}$$

Pulsars Eject Relativistic Winds

Pulsars Eject Relativistic Winds

Pulsars Eject Relativistic Winds

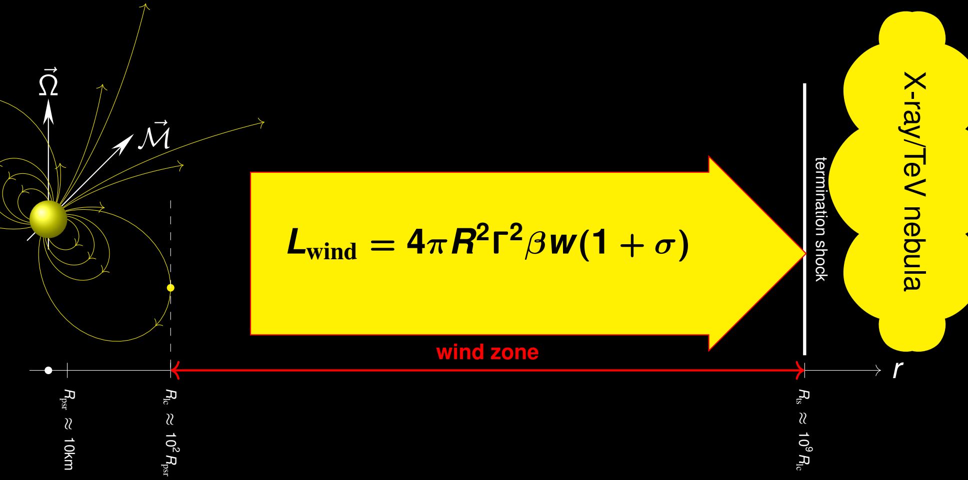

Pulsars Eject Relativistic Winds

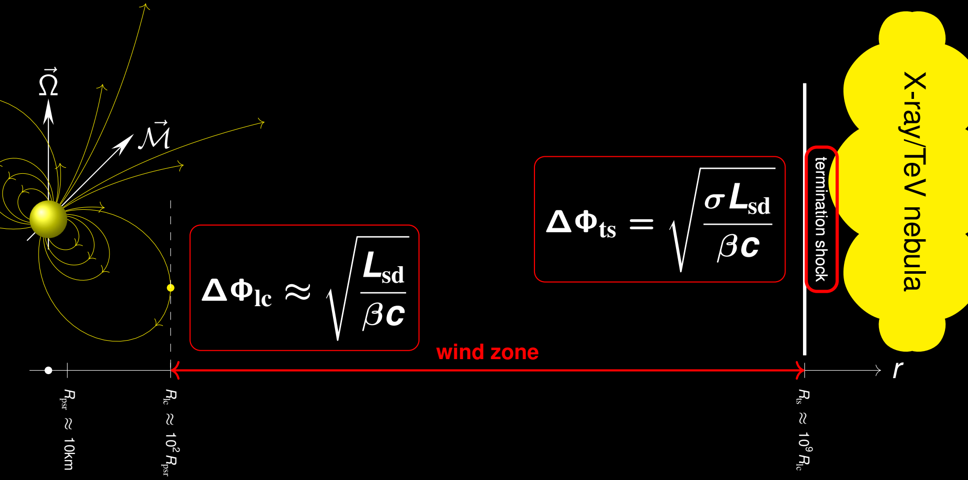

$$\Delta\Phi_{lc} \approx \sqrt{\frac{L_{sd}}{\beta c}}$$

$$\Delta\Phi_{ts} = \sqrt{\frac{\sigma L_{sd}}{\beta c}}$$

Pulsars Eject Relativistic Winds

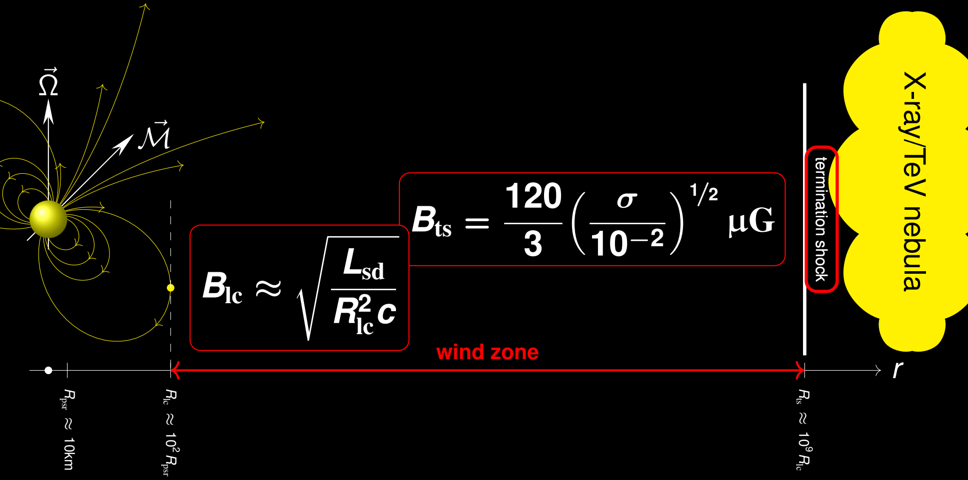

Pulsars Eject Relativistic Winds

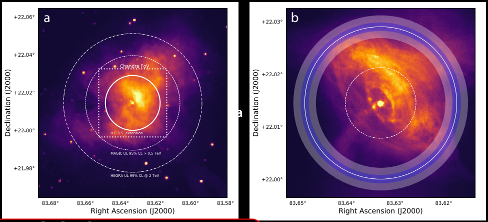

H.E.S.S. Collaboration 2019

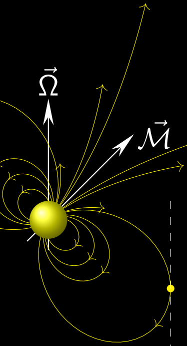

$$B_{\rm ts} = \frac{120}{3}\left(\frac{\sigma}{10^{-2}}\right)^{1/2}\ \mu\mathrm{G}$$

$$B_{\rm lc} \approx \sqrt{\frac{L_{\rm sd}}{R_{\rm lc}^2 c}}$$

σ is low: Kennel&Coroniti(1984), Aharonian&Atoyan(1995)

termination shock

wind zone

r

$R_{\rm psr} \approx 10$km

$R_{\rm lc} \approx 10^2 R_{\rm psr}$

$R_{\rm ts} \approx 10^9 R_{\rm lc}$

Crab@UHE

Spectrum Extends to 2PeV

Hillas Criterion

for $\approx$ 4 PeV electrons

$$\sqrt{\frac{\sigma L}{10^{38}\mathrm{erg/s}}} > 0.2$$

i.e. $\sigma > 0.01$ or $B > 100\mu\mathrm{G}$. It means that the synchrotron emission of PeV electrons brighter by a factor of

$$1.4 \times 10^3 \left(\frac{B}{112\mu\mathrm{G}}\right)^2$$

is that consistent with SED?

Crab@UHE

Spectrum Extends to 2PeV

Khangulyan+2020

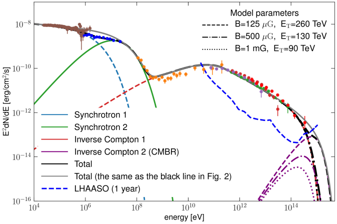

Hillas Criterion

for $\approx$ 4 PeV electrons

$$\sqrt{\frac{\sigma L}{10^{38}\mathrm{erg/s}}} > 0.2$$

i.e. $\sigma > 0.01$ or $B > 100\mu\mathrm{G}$. It means that the synchrotron emission of PeV electrons brighter by a factor of

$$1.4 \times 10^3 \left(\frac{B}{112\mu\mathrm{G}}\right)^2$$

is that consistent with SED?

Crab@UHE

Spectrum Extends to 2PeV

Hillas Criterion

for $\approx$ 4 PeV electrons

$$\sqrt{\frac{\sigma L}{10^{38}\mathrm{erg/s}}} > 0.2$$

i.e. $\sigma > 0.01$ or $B > 100\mu\mathrm{G}$. It means that the synchrotron emission of PeV electrons brighter by a factor of

$$1.4 \times 10^{3} \left(\frac{B}{112\mu\mathrm{G}}\right)^{2}$$

is that consistent with SED?

Only if magnetic field is $\approx 120\mu\mathrm{G}$. A precise measuremnt of magnetic field in the Crab Nebula? (TS region)

Khangulyan+2020

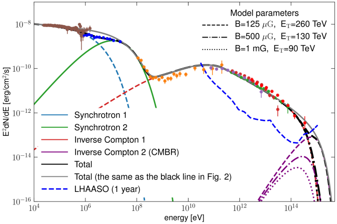

LHAASO 2021

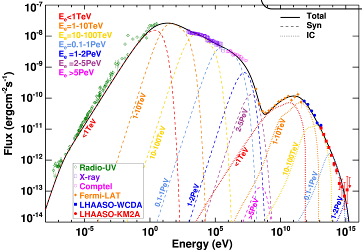

Summary

- ☞ Among the first 12 sources reported by LHAASO Col. only two do not allow association with pulsars. Three can be associated only with pulsars
- ☞ In the first LHAASO Catalogue, at least one third of the sources is associated with pusars
- ☞ The size of diffuse sources is determined by the source age for protons and cooling time for electrons (i.e., it might be easier to see lepton sources in the data)
- ☞ On the other hand, pulsar wind termination shocks seem to feature the best conditions for particle acceleration, with all constraints implying a multi PeV limits, thus it could be that PWN are indeed very efficient PeVatrons
- ☞ LHAASO data allow determing the strength of the magnetic field at the termination shock in the Crab Nebula with impressive accuracy (will we have to reconsider the “strength” of the constraints?)

Binary Systems Detected With LHAASO

- μQs were among the first source classes to be claimed to detected in the HE/VHE/UHE regime (40 years ago)
- These earlier detections were considered wrong, and little progress was done for decades
- Detection of SS433 with HAWC (2017) opened a new era in the field

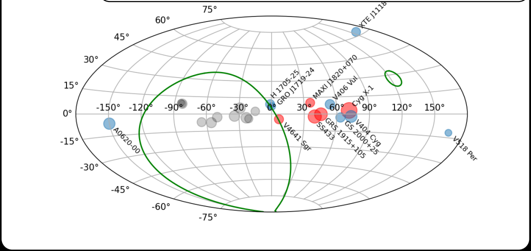

Binary system detected with LHAASO (2024)

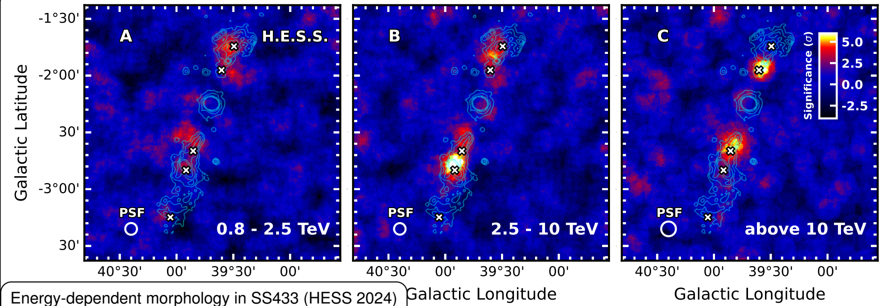

Energy-dependent morphology in SS433 (HESS 2024)